Available online at www.sciencedirect.com

SCIENCE DIRECT

Biochimica et Biophysica Acta 1668 (2005) 75–86

BIOCHIMICA ET BIOPHYSICA ACTA BBA

http://www.elsevier.com/locate/bba

The Folch–Lees proteolipid induces phase coexistence and transverse reorganization of lateral domains in myelin monolayers

C.M. Rosetti, R.G. Oliveira[1], B. Maggio*

Departamento de Química Biológica-CIQUIBIC, Facultad de Ciencias Químicas, Universidad Nacional de Córdoba, Ciudad Universitaria, 5000 Córdoba, Argentina

Received 12 August 2004; received in revised form 11 November 2004; accepted 16 November 2004
Available online 2 December 2004

Abstract

Solvent solubilized myelin membranes spread as monomolecular layers at the air–water interface show a heterogeneous pattern at all surface pressures. In order to asses the role of myelin protein and lipid components in the surface structuring we compared the topography, as seen by Brewster angle microscopy (BAM) and epifluorescence microscopy, of monolayers made from mixtures containing all myelin lipids (except gangliosides) and variable proportions of Folch–Lees proteolipid protein (PLP, the major protein component of myelin). The presence of the single PLP, in the absence of the other myelin proteins, can reproduce the surface pattern of the whole myelin extract films in a concentration-dependant manner. Moreover, a threshold mole fraction of PLP is necessary to induce the lipid–protein component reorganization leading to the appearance of a rigid (gray) phase, acting as a surface skeleton, at low surface pressures and of fractal clusters at high surface pressures. The average size of those clusters is also dependent on the PLP content in the monolayer and on the time elapsed from the moment of film spreading, as they apparently result from an irreversible lateral aggregation process. The transverse rearrangement of the monolayer occurring under compression was different in films with the highest and lowest PLP mole fractions tested.

Keywords: Monolayer; Lipid–protein interface; Phase coexistence; Folch–Lees proteolipid; Epifluorescence microscopy; Brewster angle microscopy

1. Introduction

The phenomenon of lateral phase coexistence has been conceived many years ago on the basis of calorimetric studies of reconstituted systems of lipids and proteins [1,2]. More recently, coexisting domains in different phase state could be directly observed with artificial model membrane systems (monolayers and bilayers) of different complexity [3–6]. These experiments have revealed a new level of surface organization in relation to the shapes, sizes, thickness, percolation and pattern distribution of coexisting domains. Furthermore, there are already some results pointing to an important role of the morphologic and topographic parameters for the control of the activity of lipolytic enzymes mediating the generation of lipid second messengers involved in the functional properties of membranes through signaling cascades [7–10].

There are many lines of evidence supporting that natural membranes exhibit surface domain microheterogeneity of considerable dynamics, and many indirect experiments have suggested functionality to such topography [11,12]. Hypotheses on the origin of laterally segregated membrane domains, including those generically called “rafts” on operational terms [11,13], consider that their formation can be driven by distinctive interactions among different lipid species [14]. Proteins have been mostly considered to passively partition into pre-assembled lipid domains, or specifically associate to lipids with different affinities depending on polar head group electrostatics or hydrocarbon chain matching optimization [15].

* Corresponding author. Tel.: +54 351 4334168x221; fax: +54 351 4334074.
E-mail address: bmaggio@dqb.fcq.unc.edu.ar (B. Maggio).
[1] Present address: Lehrstuhl für Biophysik E22. Department of Physik, Techischen Universität München, 85748 Garching. Germany.

0005-2736/$ - see front matter © 2004 Elsevier B.V. All rights reserved.
doi:10.1016/j.bbamem.2004.11.009

In spite of advances during the last decade, little is known about the relevant molecular parameters determining the driving potential for phase coexistence. For relatively simple binary and ternary mixtures, some correlation between spontaneous separation of phase domains and molecular features or composition has been reported. This included mismatch of the phospholipid hydrocarbon chain length [16], lateral segregation by phospholipids of glycolipid-enriched phases [17], and induction of segregated liquid-ordered phases by cholesterol [18]; however, almost nothing is known for more complex mixtures.

Alterations of the lipid and protein compositions of central nervous system myelin are related to the structural instability and dysfunction of this membrane in various human and experimental demyelinating diseases [19], and selective alterations of the content of specific lipids and proteins have been correlated to the evolution of the neurological process in autoimmune encephalomyelitis [20]. We have previously described [21] the thermodynamic–electrostatic behavior and surface topography of compositionally complex lipid–protein monolayers prepared with the whole myelin membrane at the air–water interface under conditions of continuously known intermolecular organization. From these studies it was determined that the myelin monolayer exhibited a smooth compression isotherm but with coexistence of immiscible phases at all surface pressures which involved immiscibility among some of the film components. Fluorescent immunolabeled myelin proteins and specific fluorescent ligands to charged lipid components were found to colocalize in domains segregated from the fluorescent labels associated with cholesterol and neutral or condensed lipids [5]. To further analyze the factors that may give rise to the microheterogeneous lateral organization of the myelin monolayer, we have now focused on the influence of its major protein and lipid fraction. Myelin, compared to other cell membranes, has a low protein content amounting only to about 24% by weight. About 30% of the protein fraction is represented by the myelin basic protein and about 50% by the highly hydrophobic transmembrane Folch–Lees proteolipid protein (PLP) [22]. In this work we have compared the topography of monolayers formed by all myelin components with films made from mixtures of myelin lipids and different proportions of PLP.

2. Materials and methods

2.1. Myelin fractions

Besides the total myelin extract, we isolated a solution containing almost all the myelin lipids (except for gangliosides) and a mixture of myelin lipids and PLP. The bovine spinal cord myelin was purified trough successive centrifugations in sacarose concentration gradients followed by osmotic shocks in distilled water [23], and micro-vesiculated as described elsewhere [21]. Briefly, the myelin precipitate was resuspended and dispersed in 5 vol. of phosphate buffer (1 mM pH 8) and 2 mM dithiothreitol and finally dissolved, in the same buffer, to a final protein concentration of approximately 0.2 mg/ml. The solution is gently agitated at 8 °C for 15–18 h and the precipitate obtained after centrifugation (25,000×g for 30 min) is resuspended in a small volume of the same buffer and passed five times through a 26-G syringe. To prepare the different myelin solutions to be spread as monomolecular films, the micro-vesiculated myelin [24] was fully solubilized in 19 vol. of chloroform–methanol (2:1, v/v). In this solution, all the myelin lipids and proteins remain soluble (some high molecular weight proteins, such as the Wolfgram proteins, tend to slowly aggregate with time [25]) and, if the solution is used immediately after myelin solubilization, a whole myelin monolayer can be spread that contains all its lipid and protein components; the surface behavior of such film is indistinguishable from that obtained by spreading freshly prepared micro-vesiculated myelin [21]. To continue with the isolation procedure, one-fifth volume of water was added to the extract and mixed to form two immiscible solvent phases. The mixture was centrifuged at 1000×g for 30 min to provide two sharply separated lower and upper solvent phases (representing 7:3 v/v). The lower phase (chloroform–methanol–water 86:14:1) contains essentially all the lipids (except gangliosides) and PLP as the only protein component; this phase was washed twice with a solvent solution having the same solvent composition as the upper phase (chloroform–methanol–water 3:48:47). The final lower phase is used as such to prepare films containing all the PLP but free of ganglioside, myelin basic protein, and Wolfgram proteins (all these components partition into the upper phase or remain at the two-solvent interface, which is removed). In order to obtain a total lipid fraction, the lower solvent phase was equilibrated (in proportion 1:1) with a chloroform–methanol–water (3:48:47) solution saturated with potassium citrate. In this condition, the PLP becomes insoluble and can be removed because it accumulates at the two-solvent interface [26]. The procedure is repeated three times. Subsequently, the lower phase is washed with a citrate-free upper phase (in proportion 1:1). The mole fraction of PLP remaining in the final extract is 1.1×10^{-4} as measured by standard procedures [27] after incubating the sample, previously dissolved in 0.5 N NaOH, 2.5% SDS, at room temperature for 18 h [26]. According to HPTLC (running solvent: chloroform–methanol–water 70:30:4 revealed with cupric acetate 3% orthophosphoric acid 8%) the lipid extract composition matches that of total myelin, and that of the original lower phase isolated after the initial solvent partition [21].

The composition and denomination of the different fractions that we have tested in this work are summarized as follows. Whole myelin extract contains all the lipids and protein components of myelin membranes. Lower phase extract contains all myelin lipids (except gangliosides) and

PLP (mole fraction 1.8×10^{-3}) but lacks the myelin basic protein and Wolfgram proteins. Lipid extract contains the myelin lipids (except gangliosides) and a mole fraction of 1.1×10^{-4} of PLP, which is less than 6% the PLP content of lower phase extract.

2.2. Epifluorescence and Brewster angle microscopy (BAM)

During observation and registration of video images, the surface pressure and mean molecular area of the films were measured and recorded with a KSV minithrough equipment (KSV, Helsinski, Finland) or a KIBRON microtrough (Helsinski, Finland) mounted on the stage of a Zeiss Axiovert or Axioplan (Carl Zeiss, Oberkochem, Germany) epifluorescence microscope, and/or under a miniBAM (Nanofilm technologies, NFT, Gottingem, GE), as previously described [6,28].

For BAM observations, the surface was illuminated with a 658-nm p-polarized light from a 30-mW laser diode at the Brewster angle of the bare interface (from which a minimum of reflectance is achieved). An additional p-positioned analyzer filters the residual s-component background of the reflected light collected with a standard achromat (12.5-mm diameter, 25-mm focus). When a film is spread on the aqueous subphase, it acts as a third optical medium and reflects light depending on its local thickness and refractive index.

The camera of our equipment produces a gray level signal linearly related to the light intensity for 1/500 shutter speed at least up to 160 gray level arbitrary units. The relative reflectance I can be derived (r^2=0.99)from:

$$I = -0.915\times10^{-6} + \left(4.502\times10^{-6}\right)GL \qquad (1)$$

where GL is the gray level in arbitrary units [6].

Since the laser beam profile produces an inhomogeneous illumination across the image, gray level measurements were taken in a small region of 10×10 pixels (83×83 μm) located at the center of the maximum illumination area. Gray level values are the mean value of the grayscale histogram of the square 100-pixel area measured. These values were reproducible from one experiment to another within 10 arbitrary units.

For most epifluorescence observation, films were formed from lipid or lipid–protein solutions doped with 0.25–0.5 mol% of L-α-phosphatidylethanolamine-*N*-(lyssamine rhodamine B-sulfonyl) (egg-Rho-PE) with 55% of unsaturated acyl chains (Avanti Polar Lipids). This probe is partitioned preferably in liquid-expanded phases [29]. Other probes such as L-α-phosphatidylethanolamine-*N*-(4-nitrobenzo-2-oxa-1,3-diazole) (egg-NBD-PE) with 55% of unsaturated acyl chains (Avanti Polar Lipids), 1,2-dipalmitoyl-*sn*-glycero-3-phosphatidylethanolamine-*N*-(7-nitro-2-1,3-benzoxadiazol-4-yl) (16:0 NBD-PE) (Avanti Polar Lipids) and 1,2-dipalmitoyl-*sn*-glycero-3-phosphatidylethanolamine-*N*-(lyssamine rhodamine B-sulfonyl) (16:0 Rho-PE) (Avanti Polar Lipids) were also occasionally used. After the films were spread onto a TRIS–Ca buffer pH 7,4 (10 mM Tris, 100 mM NaCl, 20 mM $CaCl_2$), at least 10 min were allowed before initiating isometric compression to permit the evaporation of the solvent. Images were captured with a CCD video camera Axiocam (Zeiss) or a Micromax camera (Princeton Instruments, Inc., USA) commanded through the Axiovision software of the Zeiss microscope or Metamorph 3.0 software (Universal Imaging Corporation, PA, USA). Objectives of 20× and 3.2× were used. All the experiments were performed at room temperature (23±2 °C).

To calculate the fractal dimension, the commercial software Benoit 1.2 (Trusoft Intl. Inc. USA) was employed. The methods effectively used to determine fractal dimension were box counting and information (entropy) dimensions [30].

3. Results

3.1. Epifluorescence and BAM

Fig. 1A shows representative images of lipid extract monolayers at different surface pressures as observed by epifluorescence and BAM. It is worth reminding that the lipid mixture contains the myelin lipids and a mole fraction of PLP protein of 1.1×10^{-4}; this is less than 6% the total PLP content of the lower phase extract. In order to compare the images seen by both techniques, it must be considered that the length of the field shown in epifluorescence micrographs is approximately one third of that in BAM micrographs (see the reference bars at the bottom of the images); thus, the latter allows a wider overview of the surface topography. On the other hand, since our BAM resolution is in the order of 20 μm, many small details are better appreciated in epifluorescence images which have a resolution in the order of 1 μm.

After the lipid extract has formed a coherent film, as indicated by the lift-off in the mean molecular area–surface pressure isotherm, the fluorescent probe "egg-Rho-PE" reveals the coexistence of two phases (Fig. 1Aa). Both of these phases are liquid as deduced from the Brownian motion of some small clusters and by the relaxed borders of the domains. The surface pattern is characterized by a fluorescent probe-enriched phase polydispersed within a percolating probe-depleted phase in regularly distributed domains which are approximately circular, although some undulating fluctuations can be observed at the domain boundaries (see Fig. 1Aa and B) suggesting a low line tension. Moreover, some larger and more elliptical domains that may reach lengths of hundreds of micrometers are also present (see insert in Fig. 1Aa). The surface pattern appears more homogeneous in BAM images (Fig. 1Af). The small round domains are under the level of resolution of our equipment but some large less reflective zones are distinguished (Fig. 1Af) that may correspond to the large

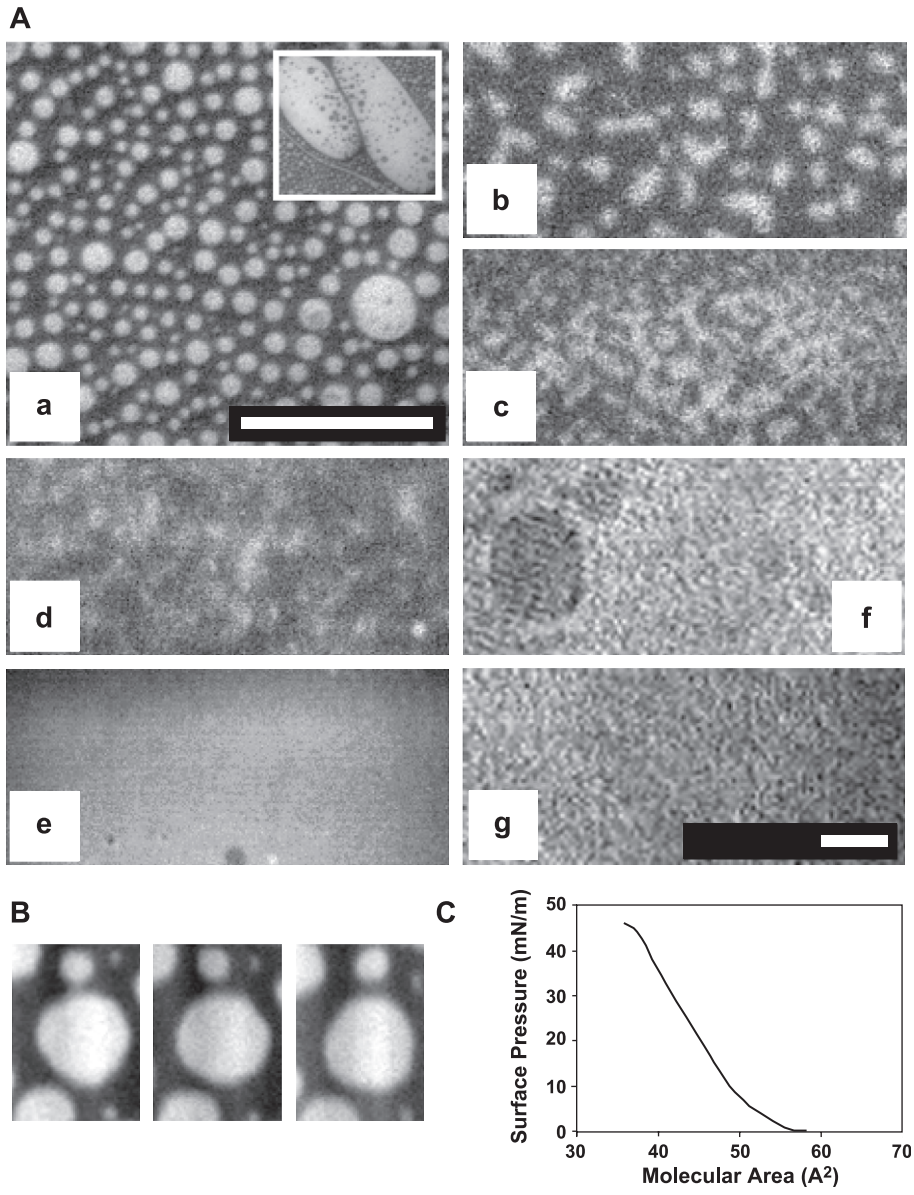

Fig. 1. (A) Representative epifluorescence (a–e) and BAM (f and g) images of lipid extract monolayers containing 0.5 mol% of egg-Rho-PE during compression at 1.5 mN/m (a and f), 2 mN/m (b and c), 2.4 mN/m (d) and 30 mN/m (e and g). The same homogeneous pattern shown in e and g is observed from merging up to collapse. Images b and c show the striped phase formed before the merging shown in image d. The fusion of bright domains leads to zones where the bright phase percolates (c). The visual field shown in the inset has 350×322 μm (the same dimensions as whole image "a") but its enlargement is the same as in the BAM images. This shows that very large fluorescent domains enclosing a small proportion of fluorescent-depleted phase are also present. The reference bars represent 150 μm. BAM images were taken at 1/50 shutter speed. (B) shows shape fluctuations of one enlarged individual fluorescent-enriched domain at 1.7 mN/m in a lipid extract monolayer. The total observation time was 6 s (from left to right an interval of 3 s separates consecutive frames). (C) shows the surface pressure–molecular area isotherm of myelin lipid extract.

fluorescent domains seen by epifluorescence (see insert of Fig. 1Aa). An inversion of contrast between both techniques occurs when the less reflective phase is the one including the fluorescent probe. We found an inversion of contrast at low surface pressures in lower phase extract films (see below).

For the lipid extract monolayers the segregation of two phases is thermodynamically favorable only over a limited range of low surface pressures and the domains merge when compressed to about 2.5 mN/m. The surface pressure–molecular area isotherm of these films does not show surface pressure-induced phase transitions that are, however, observed in the microscopy images (Fig. 1C). This can occur in multicomponent mixtures where the diversity of interactions causes loss of intermolecular cooperativity. In a previous paper, we discussed these phenomena regarding whole myelin monolayers [28]. There is some variability in relation to the phase mixing point from one lipid extract to another, and with the time elapsed between the preparation of the solution and the performance of the experiment. With freshly prepared lipids, the merging point was between 2 and 3 mN/m during the first compression while when the

monolayers were recompressed, the merging point rose to 5–6 mN/m. This last effect might result from possible oxidation of some natural lipid components of the film as reported for other mixtures [31]. Before merging, the circular shapes become unstable and stripes are progressively formed (Fig. 1Ab,c), indicating the proximity of a critical point for structural transition, as also indicated by the fluctuations of the domain boundary described above (Fig. 1B). In this scenario there are fusion phenomena between domains and changes in the connectivity of the striped phase leading to locally inverted percolation zones. After merging, the surface remains homogeneous on the basis of the partition of the fluorescent probe (Fig. 1Ae) and the surface reflectance (Fig. 1Ag) up to the collapse point.

At all surface pressures, monolayers formed with the lower phase extract and with the whole myelin extract show very similar topographies (Fig. 2A). It is worth recalling that the lower phase extract only differs from the whole myelin extract in that it lacks all the myelin proteins except for the PLP.

As reported in previous work regarding the surface topography of whole myelin monolayers, the films show coexistence of two liquid phases at low surface pressures which are organized as fluorescent probe-enriched domains within a percolating fluorescent probe-depleted phase [28]. The size and shape distribution of domains are more heterogeneous during the first compression of the film, but in successive recompressions the pattern converges to a bimodal distribution consisting of a group of regularly spaced small circular domains and larger domains which develop over lengths usually in the order of millimeter (Fig. 2A upper row of images). In BAM images the smaller domains are not resolved but the extent of the large structures can be better appreciated. At low surface pressures a third gray phase,

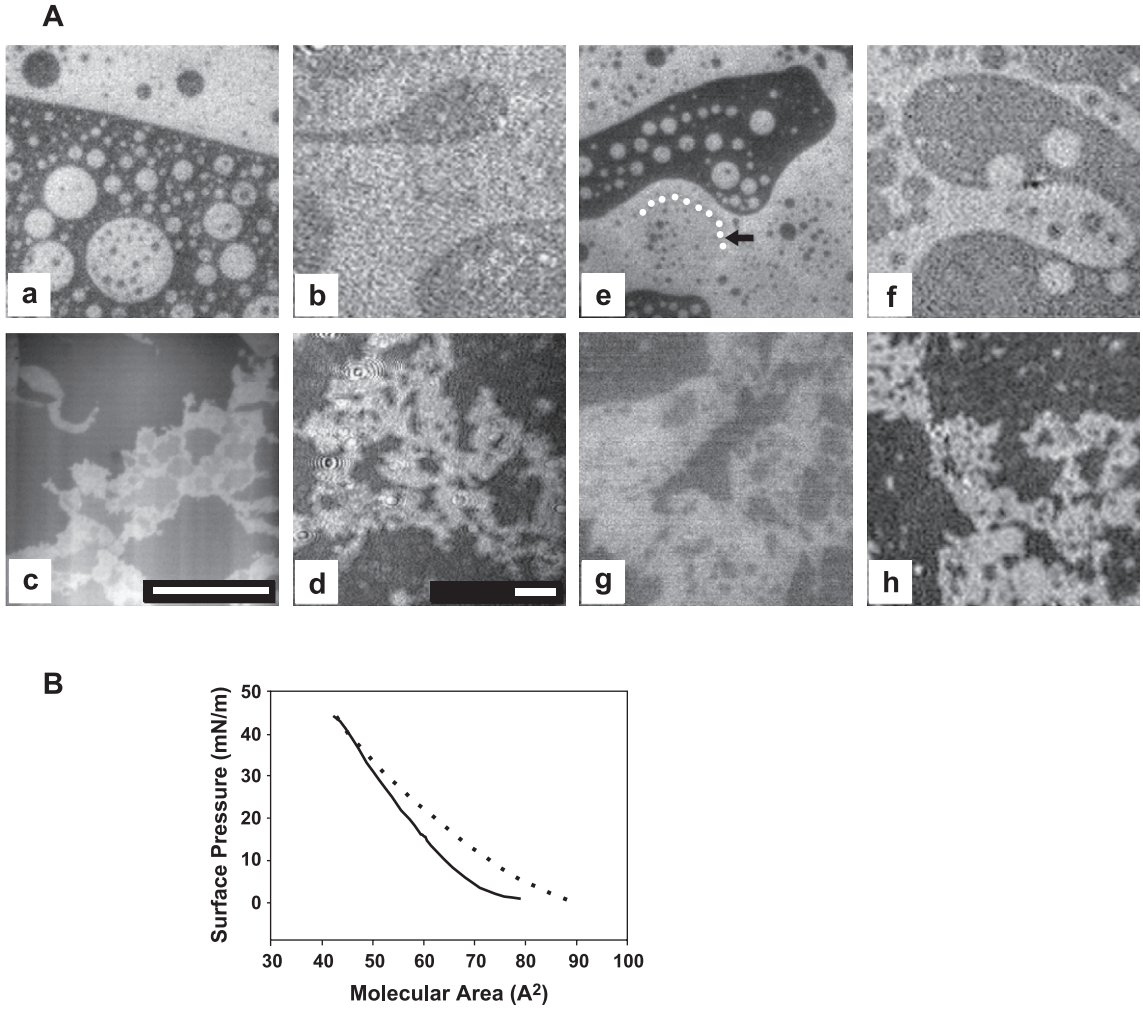

Fig. 2. (A) Representative images of whole myelin extract monolayers (a, b, c, and d) and lower phase extract monolayers (e, f, g and h) containing 0.5 mol% of egg-Rho-PE as seen by epifluorescence microscopy (a, c, e and g) and BAM (b, d, f and h). As stated in the text, the lower phase extract contains only PLP as the protein component. The upper row of images corresponds to surface pressures between 1 and 1.5 mN/m during the second compression. The arrow in image "e" is pointing to the border of the gray phase (outlined with a dotted line) that is surrounded by a rim of bright phase. The images in the bottom row were taken between 35 and 37 mN/m. The reference bars in epifluorescence and BAM images represent 150 μm. Notice that the visual field shown in BAM images is 2.8 times the visual field of epifluorescence images. The BAM images were taken with 1/50 shutter speed. (B) shows the surface pressure–molecular area isotherm of whole myelin extract (dotted line) and lower phase extract (solid line).

observed by epifluorescence and previously described in whole myelin monolayers [28], is found in lower phase extract films (Fig. 2Ae). This gray phase is not always apparent and forms irregular rigid structures inside the bright domains, excluding contacts with the dark phase (Fig. 2Ae). At high surface pressures only two phases are distinguished as shown in Fig. 2Ac, d, g and h. The structure formed by the fluorescent-enriched phase is a highly irregular network included in a dark phase of a liquid nature. Similar to the lipid extract films (see above), the surface pressure–molecular area isotherms of lower phase and whole myelin extract films (Fig. 2B and Ref. [28]) do not show surface pressure-induced phase transition correlating with the transition observed in the microscopy images. As assessed for myelin monolayers [30], the pattern observed at high surface pressures is fractal for lower phase extract films and the dimensions calculated from BAM images of whole myelin films (Fig. 2Ad) and lower phase extract films (Fig. 2Ah) were 1.71 and 1.57, respectively, calculated with box counting method, and 1.75 and 1.62 calculated with information dimension method. The self-similarity of the pattern is clearer in Fig. 3 where images of whole myelin (Fig. 3a) and lower phase extract monolayers (Fig. 3d) are shown to exhibit the same general appearance as images from inner regions of the visual field enlarged 1.7 times (Fig. 3b and e which also correspond to Fig. 2Ad and h) and three times (Fig. 3c and f). The transition between both surface patterns, rounded-to-fractal shapes, is rather gradual and involves intermediate states with progressively more elongated and thinner bright domains with increasing connectivity. The images shown in Fig. 2A are representative of the surface patterns observed below 7 mN/m (Fig. 2Aa, b, e and f) and above 25 mN/m (Fig. 2Ac, d, g and h), although these surface pressure ranges are somehow variable because, as already mentioned, the shape transitions are diffuse. It is worth noticing that at 25 mN/m, as in whole myelin monolayers [5], the inmunolabeling of PLP protein in lower phase extract films was found preferentially located in the fluorescent probe-enriched phase. According to the probe partition preferences in lipid monolayers, this would be a liquid expanded phase [29]. However, it should be pointed out that the protein-enriched fractal phase at high surface

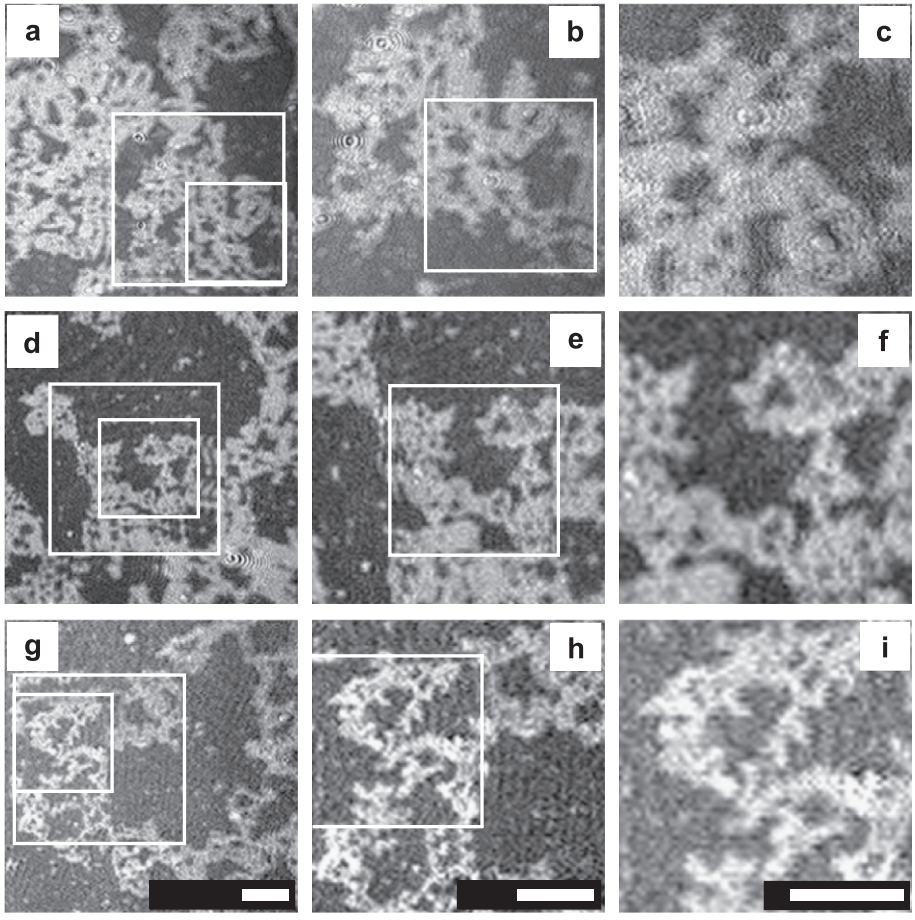

Fig. 3. Representative BAM images of monolayers of whole myelin (a, b, c), lower phase extract (d, e, f) and myelin lipids (except gangliosides) containing 5.3×10^{-4} mole fraction of PLP (g, h, i). The regions indicated by the larger squares in a, d and g are respectively enlarged in b, e and h. In turn, the regions inside the smaller squares in a, d and g are enlarged in c, f and i, respectively (notice that these images also correspond to the regions inside the squares in b, e and h). Images were taken between 35 and 37 mN/m. The reference bars correspond to 255 μm. The scale of images a and d is the same as image g. The scale of images b and e is the same as image h, and the scale of images c and f is the same as image i.

pressures shows irregular non-relaxed boundaries, suggesting a more rigid nature.

The surface pattern of monolayers containing intermediate amounts of PLP is shown in Fig. 4. These films were spread from solutions prepared by mixing various proportions of lipid extract with the lower phase extract to achieve a PLP mole fraction of 2.8×10^{-4} and 5.3×10^{-4} (15% and 30%, respectively, of the PLP content of lower phase extract). The topographic features revealed by epifluorescence in these monolayers are reminiscent of those of the films formed with whole myelin in that, at low surface pressures, the pattern converges during recompression to a bimodal distribution of small circular domains (forming quite a regular lattice) with larger domains sometimes distorted to elliptical and more irregular shapes (arrows in Fig. 4a and e); the latter are seen as less reflective domains under BAM (Fig. 4b and f). The average size of those large domains increases with the amount of PLP in the film. By epifluorescence, the largest domains show a highly noticeable inner rigid phase (gray), the relative proportions of which increase with the protein amount in the film, with non-relaxed boundaries fully surrounded ("interfacial wetting" [32]) by the brightest phase (Fig. 4a and e). The pattern described is maintained only in a narrow range of surface pressures. At around 1.5–2 mN/m the topography becomes characterized by structures of connected thin and elongated domains of irregular borders that indicate a rigid phase with non-relaxed boundary. Again, the extent of the clusters and their connectivity depend on the protein content. In films with a mole fraction of 2.8×10^{-4} of PLP, most of the domains are mostly unbranched and with a waving aspect (Fig. 4c). In BAM images they are seen as brilliant dots while the shape details fall below the resolution level of our microscope (Fig. 4d). Instead, in the films with a PLP mole fraction of 5.3×10^{-4}, branched domains of larger average size can be clearly observed by epifluorescence and BAM (Fig. 4g and h). The transition between the pattern of rounded to long thin shapes occurs primarily through the merging of at least part of the bright phase that forms the structure enclosing the gray phase. In Fig. 5, a series of epifluorescence images of films with a PLP mole fraction of 5.3×10^{-4} is shown during the expansion of the monolayer from 2.8 to 1.5 mN/m. In the sequence, the gray and irregular domains seen at higher surface pressure can be identified as the nucleating structures for the formation of the fluorescent phase acting as a structural support.

Fig. 6 shows a temporal sequence of BAM images taken at 37 mN/m showing the topography of films with a PLP mole fraction of 5.3×10^{-4}. The clusters become increasingly larger with time (Fig. 6, 1a, 1b, 1c, 1d) and their growth seems to be favored by the expansion and compression process of the monolayer (Fig. 6, 2a and 2b) The domains progressively formed have a self-similar average shape with fractal appearance. Moreover, the pattern from image 2b has a fractal dimension of 1.62 calculated with box counting method and 1.63 calculated with information dimension method. To illustrate the self-similarity of the pattern, we show in Fig. 3g–i an image of a monolayer with 5.3×10^{-4} mole fraction of PLP at 37

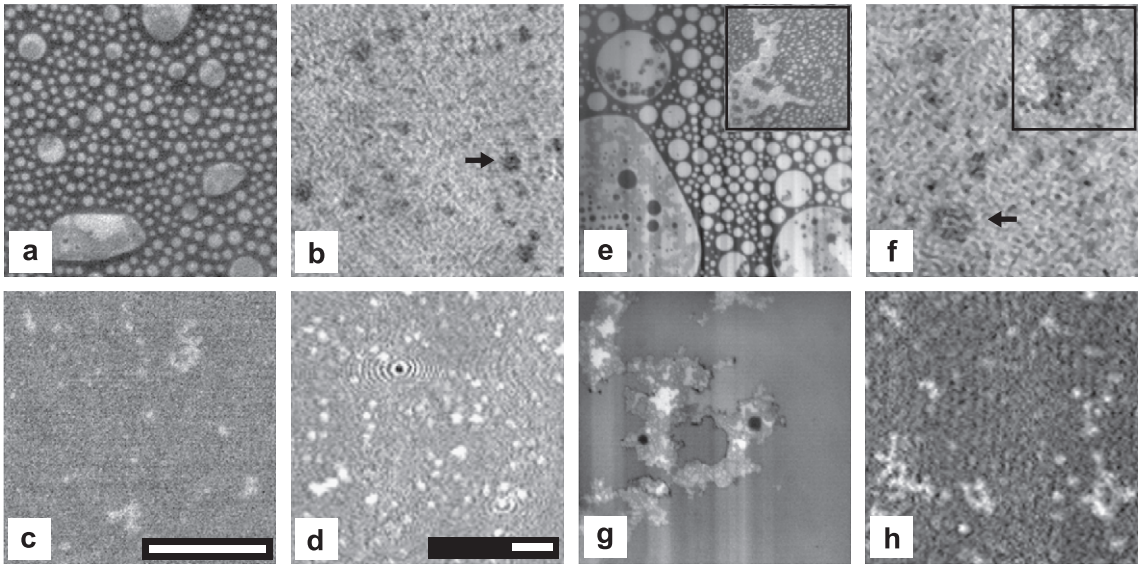

Fig. 4. Representative epifluorescence (a, c, e and g) and BAM (b, d, f and h) images of monolayers of myelin lipids containing different amounts of PLP and 0.5 mol% of egg-Rho-PE. The films shown in a, b, c and d contain a PLP mole fraction of 2.8×10^{-4}, and the films shown in e, f, g and h contain 5.3×10^{-4} mole fraction of PLP (15% and 30%, respectively, of the PLP protein content of the lower phase extract monolayers). The upper row of images corresponds to the second compression of films at surface pressures between 1 and 1.5 mN/m. The images in the bottom row are from films at surface pressures between 35 and 37 mN/m. Although BAM images at low surface pressure generally have poor contrast and many small details are lost, some large round domains can be distinguished (see the arrows). The inserts in e and f have been included to show that at low surface pressures some of the largest domains have rounded borders but very irregular shapes. The insets have the same scale as the BAM images. The reference bars represent 150 μm. The BAM images were taken with 1/50 shutter speed.

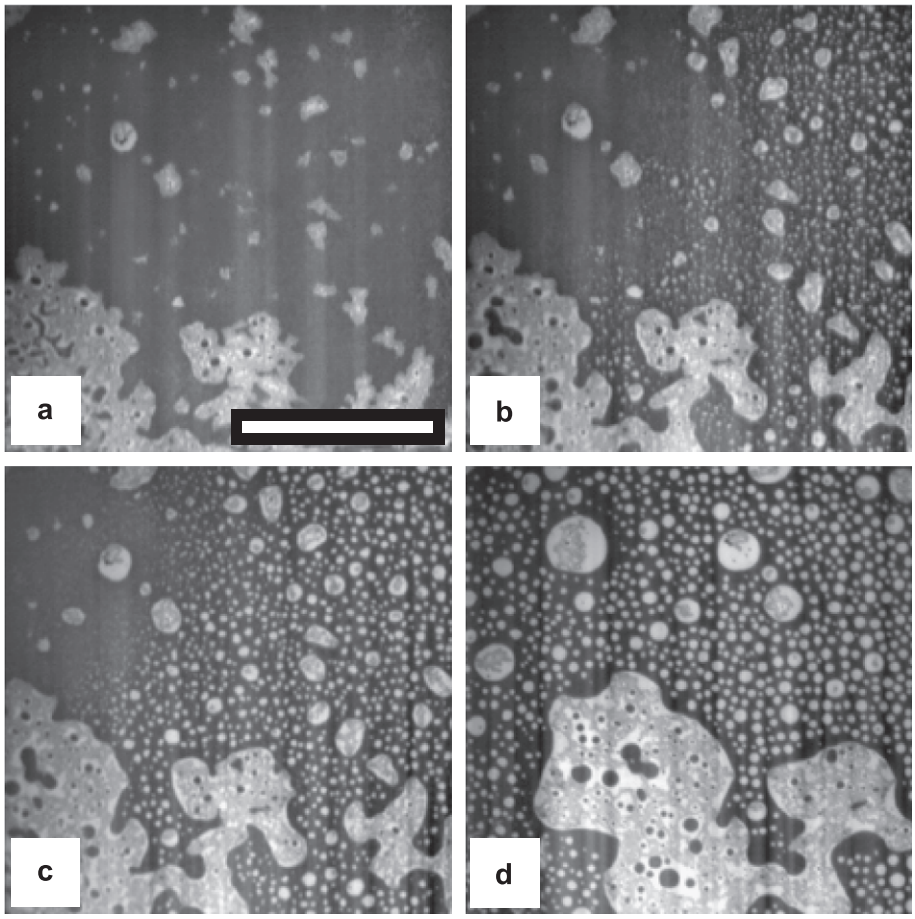

Fig. 5. Epifluorescence images of the topography of a film of myelin lipids (except gangliosides) containing 0.5 mol% of egg-Rho-PE and 5.3×10^{-4} mole fraction of PLP during the expansion at 2.8 mN/m (a), 2 mN/m (b), 1.7 mN/m (c) and 1.5 mN/m (d). The reference bars represent 150 μm.

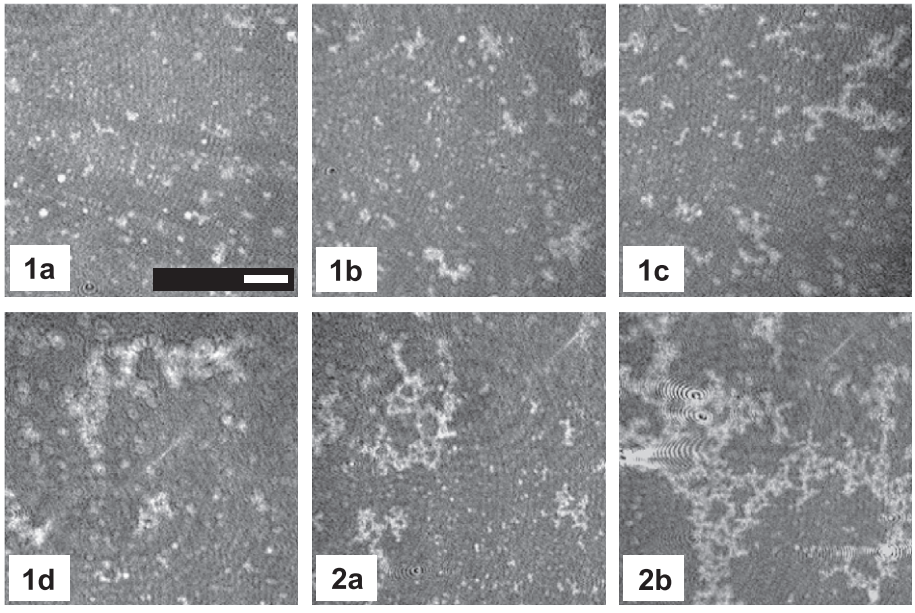

Fig. 6. Representative BAM images of a film of myelin lipids (except gangliosides) containing 5.3×10^{-4} mole fraction of PLP. The monolayer was compressed up to 37 mN/m and was left at the same surface pressure for 100 min. Images 1a, 1b, 1c and 1d are representative of the topography of the films at 2, 50, 80 and 100 min, respectively, after the target surface pressure was reached during the first compression. Images 2a and 2b show the pattern when 10 and 70 min elapsed from when the film was brought to 37 mN/m during the second compression. The reference bars represent 300 μm. BAM images were taken at 1/50 shutter speed.

mN/m from which inner regions of the visual field have been enlarged 1.7 (Fig. 3h) and 3 times (Fig. 3i). Notice that the pattern is very similar in spite of the change in the scale.

3.2. Surface reflectance

Fig. 7A shows the relative reflectance against surface pressure for films of the lipid extract and of the lower phase

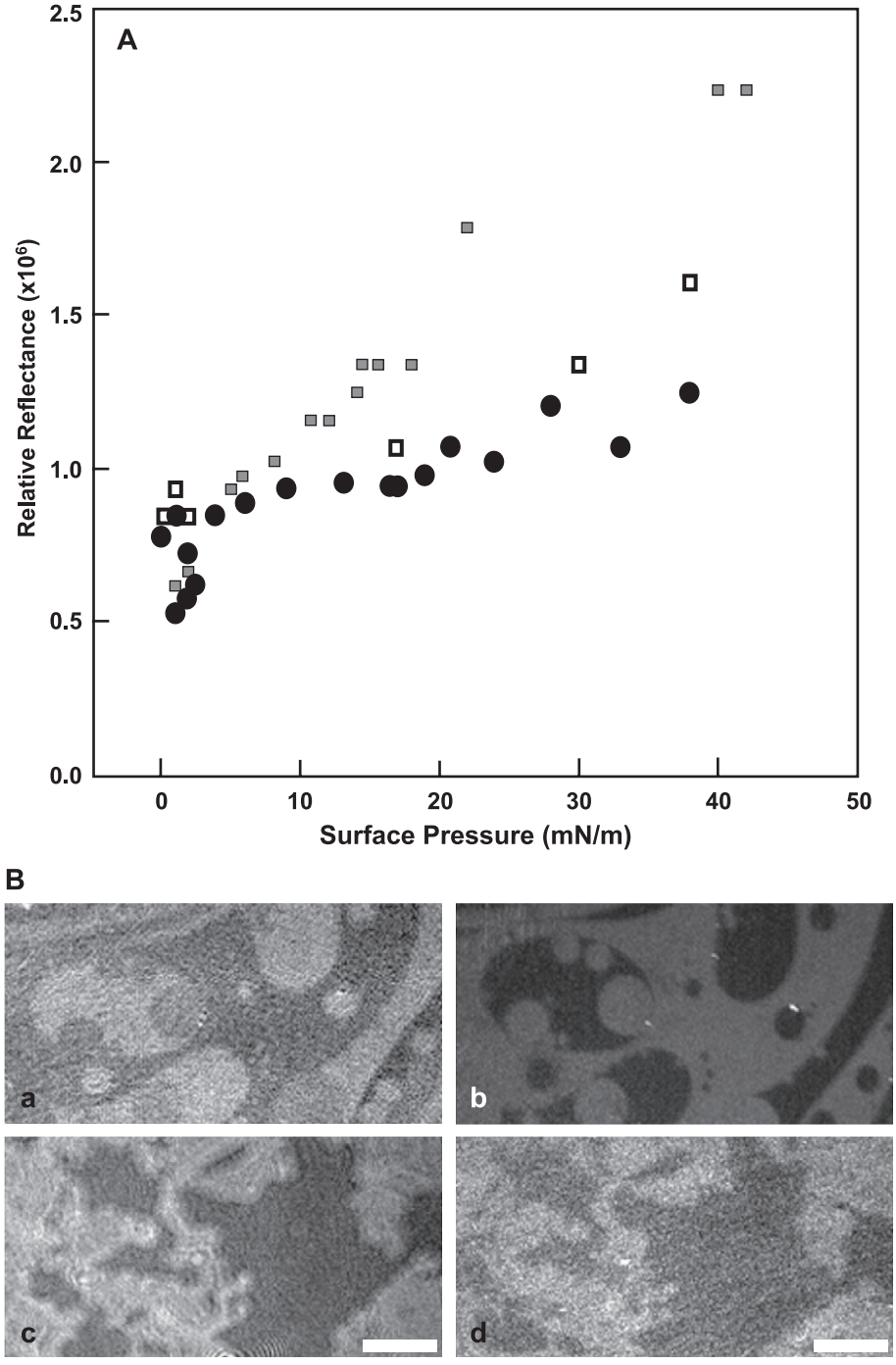

Fig. 7. (A) Plot of the relative reflectance measurements made on films of lower phase extract (■ and □) and lipid extract (●) as a function of surface pressure. The reflectance values measured in the lower phase extract film were distinctively identified when they clearly correspond to zones occupied by the probe-depleted phase (□) or the probe-enriched phase (■). In lower phase extract films, in the range of 5 to 10 mN/m, the contrast is lost in BAM images and no distinct phases are identified. The relative reflectance values were obtained using Eq. (1) from the average gray level measured in a square of 83×83 μm in the center of the illumination area of BAM images. The dispersion of values in some ranges of surface pressure is due to the flow of portions of the monolayer with different average reflectances over the area where measurements are taken. (B) Images of the same field of a monolayer of lower phase extract containing 0.5 mol% of egg-Rho-PE at 3.5 mN/m (a and b) and 20 mN/m (c and d) seen by BAM (a and c) and epifluorescence microscopy (b and d). A 3.2× objective was used to obtain the epifluorescence images. The reference bars represent 150 μm. BAM images were taken at 1/50 shutter speed.

extract. BAM images, in addition to demonstrating the lateral topography of the monolayers, may also reflect the transverse reorganization of the film domains under compression since relative reflectance values are proportional to the film optical thickness ($I \sim t^2$, where t is the film thickness). In the graph, it can be seen that the lipid extract film at low surface pressures and the lower phase extract film at low and high surface pressures show a considerable dispersion of the relative reflectance values. This is because in those surface pressure ranges there is coexistence of phases with different reflectance in the monolayer as the film flows; the relatively small area of the visual field over which the intensities are evaluated (83×83 μm) becomes randomly covered by regions with different proportions of those phases. In the lipid extract above 3 mN/m, after the surface became homogeneous by epifluorescence, the relative reflectance increases linearly and with little dispersion with the surface pressure (Fig. 7A, filled circles). On the other hand, in the lower phase extract films two different phases are identified by BAM at low and high surface pressures (Fig. 7Ba,c); these phases correspond rather accurately to the fluorescence-enriched and fluorescence-depleted phases (Fig. 7Bb,d). It can be clearly appreciated that the more reflective phase by BAM is the fluorescence-depleted phase at 3.5 mN/m but is the fluorescence-enriched phase at 20 mN/m. In Fig. 7A, the relative reflectance values mainly corresponding to the fluorescence-depleted phase are represented with open squares and the values measured in the regions covered mainly by the fluorescence-enriched phase are represented with filled squares. On this basis, the fluorescence-depleted phase shows a low increase of its relative reflectance as the film is compressed with a slope comparable to that of the lipid extract film (filled circles). On the contrary, the fluorescence-enriched phase shows a rather large variation of its relative reflectance with changes of surface pressure. The inversion of contrast among the phases occurs in the range of 5 to 10 mN/m.

4. Discussion

Our current results contribute to the elucidation of the possible roles of the lipid extract and at least one of the major myelin proteins on the topographic organization of the monomolecular films formed by the myelin components. In turn, the surface structuring is related to major topographic and compositionally driven dynamic features of the interface. Regarding the protein fraction, we determined that the presence of the single PLP is enough to reproduce the topographic surface behavior of the whole myelin extract monolayer in a manner that is dependent on the protein content. The elimination of the rest of the proteins, representing about 50% by weight of the protein fraction, does not result in major variations in the surface organization compared to the film formed by the whole myelin membrane. However, it remains to be seen whether the effect of other myelin proteins could possibly be redundant in also reproducing (in the absence of PLP) the characteristic pattern and surface pressure-dependent organization found in the whole myelin film that is not present in lipid extract monolayers; this is currently under study.

Mixtures containing the myelin lipids (except gangliosides) and a small amount of PLP (mole fraction of 1.1×10^{-4}), denominated as lipid extract, show a pattern consisting of only two coexisting liquid phases over a narrow range of low surface pressures. The full merging of the liquid phases (as reported by the fluorescent probe partitioning) is favored when the surface pressure is raised above 2–3 mN/m. The formation of a third gray phase, which is found embedded within the bright domains, is only observed in films containing more than 2.8×10^{-4} mole fraction of PLP and its extent is correlated with the content of PLP in the monolayer. Moreover, the gray phase seems to originate on the PLP-enriched domains found at high surface pressures (see Fig. 5). On the other hand, from the comparison of the topography of the films tested, over the range of surface pressures where all the monolayers show some kind of surface pattern (up to 2–3mN/m), it is clear that the presence of PLP markedly influences the topographic features regarding the size and shape distribution of domains in a manner dependent on the protein proportion in the film (see Figs. 1A, 2A and 4).

The surface pattern found at low surface pressures in all the studied monolayers resembles that described in a number of binary and ternary mixtures containing cholesterol together with glycerophospholipids and/or sphingolipids [4]. Cholesterol is known to determine phase segregation of cholesterol-enriched liquid-ordered phases and phospholipid-enriched liquid-disordered phases [33,34]. In myelin monolayers, phospholipids and cholesterol constitute more than 80% of the lipid fraction (on a molar basis), with cholesterol representing about 42%, a percentage at which segregation of the liquid-ordered phase is present in other systems [35]. We previously identified, in whole myelin monolayers, the fluorescent probe-depleted domains as a cholesterol-enriched phase [5]. In this work, we have determined that in monolayers prepared with the lower phase extract the fluorescence-depleted phase also corresponds to a cholesterol-enriched phase (not shown). Other reconstituted films prepared with natural lipid mixtures mimicking the lipid composition of cell membranes have also been reported to show immiscible cholesterol-enriched and cholesterol-depleted liquid phases [36]. In those experiments, as in our monolayers formed with the lipid extract, the coexisting phases undergo surface mixing under compression beyond a critical surface pressure point. These phenomena arise from the marked condensation of the mean molecular area that cholesterol spontaneously induces on its neighboring molecules, thus thermodynamically favoring phase segregation at low, but not at high, surface pressures [3]. In addition, the topographic features of the lipid extract films near the phase

merging point (see the striped phase and border fluctuations in Fig. 1Ab,c and B, respectively) reveal that these monolayers are at, or near, a critical point similar to that observed in other complex mixtures of lipids mimicking cell membranes [36].

The heterogeneous topography of whole myelin extract monolayers at high surface pressures appears determined by the single presence of PLP in the film together with myelin lipids. A threshold PLP mole fraction among 1.1×10^{-4} and 2.8×10^{-4} is required to induce a surface pattern of thin and elongated irregular domains. The clusters observed by BAM formed soon after the first compression have a length extent that increases with the proportion of PLP in the film (compare Figs. 2Ah and 4d,h) and, at least in films with a mole fraction of PLP of 5.3×10^{-4}, the clusters continue to grow with time forming self-similar fractal structures without an equilibrium size. Moreover, the spontaneous cluster aggregation to form the fractal domains is an apparently irreversible process. When the film is expanded the clusters remain integrally associated and form the starting support for the formation of the gray phase and the nucleation of newly formed fluorescent liquid phase under expansion. On successive recompressions the average size of the clusters at high surface pressures is further increased. In the lower phase extract films and whole myelin extract monolayers the PLP has been localized in the fractal clusters. In previous work [5] ganglioside GM1 together with myelin basic protein was found to colocalize with PLP in the fractal clusters of whole myelin extract monolayers. Moreover, some preliminary results indicate an effect of the hydrocarbon chains saturation on the partition of lipidic fluorescent probes among the different phases in lower phase extract films. At high surface pressure, the probes egg-NBD-PE and egg-Rho-PE having unsaturations in their hydrocarbon chains preferably partition into the fractal domains. By contrast, for C16-Rho-PE and C16-NBD-PE, having the same polar head group but all saturated hydrocarbon chains, the partition in the cholesterol-enriched phase is favored. This suggests that, although a major factor to induce formation of the domains at high surface pressures is the aggregation of PLP protein (the thermodynamic tendency of myelin lipids at those pressures is to mix homogeneously), there are lipids that would preferably partition into the fractal phase, a tendency driven by some molecular structural properties (as may be the hydrocarbon chain saturation). Thus, the aggregation of the PLP protein appears to provide a thermodynamic basis for the formation of domains at high surface pressures although the underlying protein–protein and/or lipid–protein interactions involved remain unknown. On the other hand, the fractal arrangement of the domains formed is indicative that they may organize through a non-equilibrium process. The formation of fractal structures has been experimentally observed and theoretically described for diffusively aggregating spherical particles [37] and theoretical simulations of photosystems aggregation in membranes have predicted ramified fractal-like structures under certain conditions [38]. In those cases, the type of domain surface structure organized is expected to depend on the balance of the interaction energy among particles and the thermal energy. In our system, the factors that contribute to the formation of a fractal pattern at high surface pressures remain to be identified but a strong interaction between PLP protein units could lead to a non-equilibrium aggregation into fractal domains.

As could be expected, there is also a large difference in the transverse structuring of the monolayer along the plane perpendicular to the interface that is dependent on the PLP content. In the lipid fraction after merging (above 2–3 mN/m) and in the fluorescent probe-depleted phase of the films formed with the lower phase extract, only small variations of the relative reflectance occur with changes of surface pressure. This is expected because the presence of cholesterol induces, by itself, a conformational order in the lipid hydrocarbon chains which acquire concomitantly a more closely packed state. On the contrary, the phase containing the PLP in the lower phase extract films undergoes a marked rearrangement with the surface pressure. As described for many proteins and polymers at interfaces at low surface pressures, the PLP may adopt an expanded conformation [39–41]. At higher surface pressures, the calculated mean molecular area range occupied by PLP (17 to 13 nm^2 between 20 and 40 mN/m) is in keeping with the adoption of a closed molecular packing consistent with a more condensed erect state.

In summary, in the topographic organization of whole myelin monolayers two overlapping contributions were identified. The lipid extract containing PLP at a mole fraction of 1.1×10^{-4} induces the coexistence of liquid phases at low surface pressures leading to a pattern of domains with relaxed boundaries. The PLP protein induces through the reorganization of the lipid–protein components the appearance of a rigid (gray) phase that, acting as a sort of surface skeleton, determines the shapes, sizes and dynamic behavior of domains. The heterogeneous topography at surface pressures beyond a few mN/m (2–3 mN/m) is a property acquired by the monolayer only when PLP, above some threshold proportion, is present in the films leading to a fractal pattern that is originated as an irreversible domain aggregation process. The PLP by itself, when mixed with the lipid extract, is capable of reproducing the surface topography of the whole myelin monolayer in a concentration-dependent manner.

Acknowledgments

This work was supported by SECyT-UNC, CONICET, FONCYT and Fundación Antorchas. C.M.R is a postgraduate fellow and B.M. is Principal Career Investigator of CONICET. R.G.O was a posdoctoral fellow of FONCyT and at present is an A. von Humboldt posdoctoral fellow at

Lehrstuhl für Biophysik E22, Department of Physik, Techischen Universität München, Garching, Germany.

References

[1] M.C. Phillips, B.D. Ladbrooke, D. Chapman, Molecular interactions in mixed lecithin systems, Biochim. Biophys. Acta 196 (1970) 35–44.
[2] O.H. Griffith, P. Jost, R.A. Capaldi, G. Vanderkooi, Boundary lipid and fluid bilayer regions in cytochrome oxidase model membranes, Ann. N.Y. Acad. Sci. 222 (1973) 561–573.
[3] H.M. McConnell, Structures and transitions in lipid monolayers at the air–water interface, Annu. Rev. Phys. Chem. 42 (1991) 171–195.
[4] C. Dietrich, L.A. Bagatolli, Z.N. Volovyk, N.L. Thompson, M. Levi, K. Jacobson, E. Gratton, Lipid rafts reconstituted in model membranes, Biophys. J. 80 (2001) 1417–1428.
[5] R.G. Oliveira, B. Maggio, Composition domain immiscibility in whole myelin monolayers at the air–water interface and Langmuir–Blodgett films, Biochim. Biophys. Acta 1561 (2002) 238–250.
[6] C.M. Rosetti, R.G. Oliveira, B. Maggio, Reflectance and topography of glycosphingolipid monolayers at the air–water interface, Langmuir 19 (2003) 377–384.
[7] M.L. Fanani, S. Hartel, R.G. Oliveira, B. Maggio, Bidirectional control of sphingomyelinase activity and surface topography in lipid monolayers, Biophys. J. 83 (2002) 3416–3424.
[8] I.P. Sugar, N.K. Mizuno, M.M. Momsen, H.L. Brockman, Lipid lateral organization in fluid interfaces controls the rate of colipase association, Biophys. J. 81 (2001) 3387–3397.
[9] B. Maggio, Control by ganglioside GD1a of PLA2 activity through modulation of the lamellar–hexagonal (HII) phase transition, Mol. Membr. Biol. 13 (1996) 109–112.
[10] G. Basáñez, G.D. Fidelio, F.M. Goñi, B. Maggio, A. Alonso, Dual inhibitory effect of gangliosides on phospholipase C-promoted fusion of lipidic vesicles, Biochemistry 35 (1996) 7506–7513.
[11] M. Edidin, Shrinking patches and slippery rafts: scales of domains in the plasma membrane, Trends Cell Biol. 11 (2001) 492–496.
[12] G. Vereb, J. Matko, G. Vamosi, S.M. Ibrahim, E. Magyar, S. Varga, J. Szollosi, A. Jenei, R. Gaspar Jr., T.A. Waldmann, S. Damjanovich, Cholesterol-dependent clustering of IL-2Ralpha and its colocalization with HLA and CD48 on T lymphoma cells suggest their functional association with lipid rafts, Proc. Natl. Acad. Sci. U. S. A. 97 (2000) 6013–6018.
[13] B. Maggio, D.C. Carrer, M.L. Fanani, R.G. Oliveira, C.M. Rosetti, Interfacial behavior of glycosphingolipids and chemically related sphingolipids, Curr. Opin. Colloid Interface Sci. 8 (2004) 448–458.
[14] T.Y. Wang, J.R. Silvius, Different sphingolipids show differential partitioning into sphingolipid/cholesterol-rich domains in lipid bilayers, Biophys. J. 79 (2000) 1414–1478.
[15] O.G. Mouritsen, M. Bloom, Mattress model of lipid–protein interactions in membranes, Biophys. J. 46 (1984) 141–153.
[16] J.L. Slater, C.H. Huang, I.W. Levin, Interdigitated bilayer packing motifs: Raman spectroscopic studies of the eutectic phase behavior of the 1-stearoyl-2-caprylphosphatidylcholine/dimyristoylphosphatidylcholine binary mixture, Biochim. Biophys. Acta 1106 (1992) 242–250.
[17] B. Maggio, T. Ariga, J.M. Sturtevant, R.K. Yu, Thermotropic behavior of binary mixtures of dipalmitoylphosphatidylcholine and glycosphingolipids in aqueous dispersions, Biochim. Biophys. Acta 818 (1985) 1–12.
[18] S.L. Veatch, I.V. Polozov, K. Gawrisch, S.L. Keller, Liquid domains in vesicles investigated by NMR and fluorescence microscopy, Biophys. J. 86 (2004) 2910–2922.
[19] M.E. Smith, J.A. Benjamin, Model systems for study of perturbations of myelin metabolism, in: P. Morell (Ed.), Myelin, Plenum Press, New York, 1984, pp. 441–488.
[20] B. Maggio, F.A. Cumar, Experimental Allergic Encephalomyelitis: dissociation of neurological symptoms from lipid alterations in the brain, Nature 253 (1975) 364–365.
[21] R.G. Oliveira, R.O. Calderon, B. Maggio, Surface behavior of myelin monolayers, Biochim. Biophys. Acta 1370 (1998) 127–137.
[22] M.B. Lees, S.W. Brostoff, Proteins of myelin, in: P. Morell (Ed.), Myelin, Plenum Press, New York, 1984, pp. 441–488.
[23] J.E. Haley, F.G. Samuels, R.W. Ledeen, Studies of myelin purity in relation to axonal contamination, Cell. Mol. Neurobiol. 1 (1981) 175–178.
[24] C. Wütrich, A.J. Steck, A permeability change of myelin membrane vesicles toward cations is induced by MgATP but not by phosphorylation of myelin basic protein, Biochim. Biophys. Acta 640 (1981) 195–206.
[25] F. Gonzalez-Sastre, The protein composition of isolated myelin, J. Neurochem. 17 (1970) 1049–1056.
[26] M.L. Lees, D.J. Sakura, Research methods in neurochemistry, in: N. Marks, R. Rodnight (Eds.), Preparation of Proteolipids, Plenum Press, New York, 1978.
[27] O.H. Lowry, N.J. Rosebrough, A.L. Farr, R.J. Randall, Protein measurements with the Folin phenol reagent, J. Biol. Chem. 193 (1951) 265–275.
[28] R.G. Oliveira, B. Maggio, Epifluorescence microscopy of surface domain microheterogeneity in myelin monolayers at the air–water interface, Neurochem. Res. 25 (2000) 77–86.
[29] H.M. McConnell, Periodic structures in lipid monolayer phase transition, Proc. Natl. Acad. Sci. U. S. A. 81 (1984) 3249–3253.
[30] R.G. Oliveira, M. Tanaka, B. Maggio, Many length scales surface fractality in monomolecular films of lipids and proteins extracted form whole myelin, J. Struct. Biol. (in press).
[31] D.J. Benvegnu, H.M. McConnell, Surface dipole densities in lipid monolayers, J. Phys. Chem. 97 (1993) 6686–6691.
[32] O.G. Mouritsen, K. Jørgensen, Dynamical order and disorder in lipid bilayers, Chem. Phys. Lipids 73 (1994) 3–25.
[33] J.H. Ipsen, G. Karlstrom, O.G. Mouritsen, H. Wennerstrom, M.J. Zuckermann, Phase equilibria in the phosphatidylcholine–cholesterol system, Biochim. Biophys. Acta 905 (1987) 162–172.
[34] L.A. Worthman, K. Nag, P.J. Davis, K.M. Keough, Cholesterol in condensed and fluid PC monolayers studied by epifluorescence microscopy, Biophys. J. 72 (1997) 2569–2580.
[35] H. Möhwald, Phospholipid monolayers, in: Structure and Dynamics of Membranes: From Cells to Vesicles, vol. 1, Elsevier, Amsterdam, 1995, pp. 161–211.
[36] S.L. Keller, W.H. Pitcher III, W.H. Huestis, H.M. McConnell, Red blood cell lipids form immiscible liquids, Phys. Rev. Lett. 81 (1998) 5019–5022.
[37] W.K.C. Poon, M.D. Haw, Mesoscopic structure formation in colloidal aggregation and gelation, Adv. Colloid Interface Sci. 73 (1997) 71–126.
[38] A. Borodich, I. Rojdestvenski, M. Cottam, Lateral heterogeneity of photosystems in thylakoid membranes studied by Brownian dynamics simulations, Biophys. J. 85 (2003) 774–789.
[39] G.D. Fidelio, B. Maggio, F.A. Cumar, Interaction of soluble and membrane proteins with monolayers of glycosphingolipids, Biochem. J. 203 (1982) 717–725.
[40] G.A. Borioli, B.L. Caputto, B. Maggio, c-Fos is surface active and interacts differentially with phospholipid monolayers, Biochem. Biophys. Res. Commun. 280 (2001) 9–13.
[41] S. Angeletti, B. Maggio, S. Genti-Raimondi, Surface activity and interaction of StarD7 with phospholipid monolayers, Biochem. Biophys. Res. Commun. 314 (2004) 181–185.